T.G.Elizarova, I.S.Kalachinskaya, Yu.V.Sheretov

Separating Flow Behind a Back-Step. Part I. Quasi-Hydrodynamic Equations and Computation of a Laminar Flow

We demonstrate the results of the numerical modelling of a plane two-dimensional viscous incompressible flow in a channel with a back-step. As a mathematical model we take equations for a incompressible flow based on the quasi-hydrodynamic (QHD) equations. We present a phenomenological derivation of the QHD equations and show a relation of these equations to the Navier-Stokes system. We test the proposed numerical algorithm by computing of certain laminar flows.

1   Introduction

The paper is devoted to the numerical modelling of the viscous incompressible flow behind the back-step in the channel with a sudden broadening. The quasi-hydrodynamic (QHD) system of equations is used as a mathematical model. [1], [2].

In the second part of our paper we discuss the derivation of the QHD equations and their relation to the Navier-Stokes equations. The QHD equations broaden the possibilities of the classical Navier-Stokes model in description of the viscous compressible gas flows. When the Navier-Stokes equations are applicable, the additional dissipation of the QHD equations makes little influence on the solutions, but provides the stability of numerical computations. In certain cases of weakly rarified flows the QHD equations give the solution that describes experimental data better than the Navier-Stokes model [3].

Probation of the QHD equations for computing the incompressible liquid flows and for the problems of thermal and thermocapillar convection was carried out in [4]–[7]. In particular, it was shown that the QHD equations are effective for modelling of nonstationary flows [6].

The size of the separation zone behind the step is a sensitive characteristic feature of laminar flows, which strongly depends on the flow velocity and on the geometry of the region considered in the problem. Analytical expression for the dependence of the separation zone's length on the Reynolds number and the relative height of the step for two-dimensional flows is given, for example, in [8]. The length of the separation zone grows almost linearly with the increasing of the Reynolds number. Laminar flows behind the back step are well simulated numerically and the results of two-dimensional computations of different authors are in a good agreement with experimental data [8]–[11]. It allows us to use this problem as a test for probation of new numerical algorithms.

In this paper we present the computations of the laminar flows in comparison with the previously published results. Data obtained from literature is used for evaluating the robustness and the accuracy of the numerical algorithm for computing the flow behind the step, which is based on the QHD equations. In the continuation of this paper (Part II) the method proposed here is applied to the numerical investigation of turbulent flows behind the step.

2   Mathematical model

In this section we describe the physical principles that form the basis for the phenomenological derivation of the new quasi-hydrodynamic (QHD)system of equations. Using time-space averaging for introducing the principal hydrodynamic values – density, velocity and temperature – is the essential and fundamental feature that distinguishes our method from the Navier-Stokes theory, where hydrodynamic values are introduced based on space averaging.

2.1 Integral conservation laws

Let us consider an inertial Cartesian coordinate system (x_1, x_2, x_3) in the Euclidian space $R_{\vec{x}}^3$. Let $(\vec{e}_1, \vec{e}_2, \vec{e}_3)$ be the corresponding orthonormal basis of unit vectors and let us denote time as t. We shall use the following standard notation for the variables describing the viscous compressible thermoconducting flow: $\rho = \rho(\vec{x}, t)$ – density, $\vec{u} = \vec{u}(\vec{x}, t)$ – velocity, $p = p(\vec{x}, t)$ – pressure, $\varepsilon = \varepsilon(\vec{x}, t)$ – specific internal energy, $T = T(\vec{x}, t)$ – temperature, $s = s(\vec{x}, t)$ – specific entropy.

Suppose that the medium is two-parametric, that is, only two out of five thermodynamical parameters ρ, p, ε, T, s are independent, and we are given by the state equations

$$p = p(\rho, T), \quad \varepsilon = \varepsilon(\rho, T), \quad s = s(\rho, T). \tag{1}$$

Let $\vec{F} = \vec{F}(\vec{x}, t)$ be the mass density of external forces. For example, in case of the liquid in the gravitational field of the Earth it will be $\vec{F} = \vec{g}$, where $\vec{g}$ is the gravity acceleration.

Our first postulate is the law of conservation of mass in the following form:

$$\frac{\partial \rho}{\partial t} + div \tilde{j}_m = 0. \tag{2}$$

We suppose that the mass flux density vector $\vec{j}_m = \vec{j}_m(\vec{x}, t)$ is defined in every point $\vec{x}$ of the flow in every moment of time t. In the region occupied by the flow we take an arbitrary moving material volume $V = V(t)$ with the smooth surface $\Sigma = \Sigma(t)$, oriented with the field of external normal unit vectors $\vec{n}$. We also suppose that the volume $V(t)$ originates from the volume $V_0 = V(t_0)$, where t_0 is the initial moment of time, by continuous deformation, caused by the motion of particles V_0 along the trajectories, determined by the vector field $\vec{j}_m/\rho$. Using the well-known [12] Euler–Liouville identity

$$\frac{d}{dt} \int_V \varphi dV = \int_V [D\varphi + \varphi div(\tilde{j}_m/\rho)] dV, \tag{3}$$

where $\varphi = \varphi(\vec{x}, t)$ is a certain continuously differentiable scalar or vector field, dV is a volume element in $R_{\vec{x}}^3$ and $D = \partial/\partial t + (\vec{j}_m/\rho) \cdot \vec{\nabla}$ is the differential operator, we present the law of conservation of mass (2) in the integral form:

$$\frac{d}{dt} \int_V \rho dV = 0. \tag{4}$$

The second postulate is the law of conservation of momentum

$$\frac{d}{dt} \int_V (\rho \vec{u}) dV = \int_V \rho \vec{F} dV + \iint_\Sigma (\vec{n} \cdot P) d\Sigma, \tag{5}$$

where $d\Sigma$ is the element of the surface Σ in the vicinity of the unit vector $\vec{n}$. The rate of variation of the momentum in the volume V equals to the sum of all forces applied to it. The first integral in the right hand side of (5) is a volume force caused by the external field; the second stands for the forces, caused by pressure and internal viscous friction, that are applied to the surface Σ. The variable $P = P(\vec{x}, t)$ is called the tensor of internal tensions. The symbol $(\vec{n} \cdot P)$ means the contraction (dot product) of the vector $\vec{n}$ and the second rank tensor P with respect to the first index of the tensor. Respectively, $(P \cdot \vec{n})$ means that the contraction of P and $\vec{n}$ is done with respect to the second index of P. If the tensor P is symmetric, then $(\vec{n} \cdot P) = (P \cdot \vec{n})$.

The third postulate is the law of conservation of the total energy

$$\frac{d}{dt} \int_V \rho \left(\frac{\vec{u}^2}{2} + \varepsilon \right) dV = \int_V (\vec{j}_m \cdot \vec{F}) dV + \iint_\Sigma (\vec{A} \cdot \vec{n}) d\Sigma - \iint_\Sigma (\vec{q} \cdot \vec{n}) d\Sigma. \tag{6}$$

Here the first integral in the right hand side of (6) equals to the capacity of the external volume forces that are applied to the volume V; the second is understood as the capacity of the surface forces of the pressure and the internal viscous stress. The last term in (6) describes the influx of energy in a single unit of time through the surface Σ due to the processes of the heat transfer. Actual expressions for the vector fields $\vec{A} = \vec{A}(\vec{x}, t)$ and $\vec{q} = \vec{q}(\vec{x}, t)$ will be given below.

The fourth postulate expresses the law of conservation of the moment of momentum:

$$\frac{d}{dt}\int_V [\vec{x} \times (\rho\vec{u})]dV = \int_V [\vec{x} \times \rho\vec{F}]dV + \int\int_\Sigma [\vec{x} \times (\vec{n} \cdot P)]d\Sigma. \tag{7}$$

It is presented in its classical form. Internal moments and the distributed mass and surface pairs are not taken into consideration. The symbol $\times$ denotes the cross product of two vectors.

Our fifth postulate is the second law of thermodynamics. It looks as follows:

$$\frac{d}{dt}\int_V (\rho s)dV = -\int\int_\Sigma \frac{(\vec{q}\cdot\vec{n})}{T}d\Sigma + \int_V XdV. \tag{8}$$

The surface integral in the right hand side (8) defines the rate of the variation of entropy in the volume V due to the thermal flux. It may be both positive or negative. The last integral is always non-negative: it gives the production of entropy due to the internal irreversible processes.

2.2 Transfer to differential equations

Just like in the case of the Navier–Stokes system [12], for the transfer from the integral relations (4)–(8) to the corresponding differential ones we use the Liouville formula (3) for differentiating the integral over the moving material volume. Doing it, we shall suppose that all the principal macroscopic parameters of the medium are sufficiently smooth functions of time and spatial coordinates. Taking in consideration that the volume V is arbitrary, we obtain differential equations for the balances of the mass

$$\frac{\partial\rho}{\partial t} + div\tilde{j}_m = 0, \tag{9}$$

of the momentum

$$\frac{\partial(\rho\vec{u})}{\partial t} + div(\tilde{j}_m \otimes \tilde{u}) = \rho\tilde{F} + divP, \tag{10}$$

of the total energy

$$\frac{\partial}{\partial t}\Big[\rho\Big(\frac{\vec{u}^2}{2} + \varepsilon\Big)\Big] + div\Big[\tilde{j}_m\Big(\frac{\tilde{u}^2}{2} + \varepsilon\Big)\Big] = (\tilde{j}_m \cdot \tilde{F}) + div\tilde{A} - div\tilde{q}, \tag{11}$$

of the moment of momentum

$$\frac{\partial}{\partial t}[\vec{x} \times \rho\vec{u}] + div(\tilde{j}_m \otimes [\tilde{x} \times \tilde{u}]) = [\tilde{x} \times \rho\tilde{F}] + \frac{\partial}{\partial x_i}[\tilde{x} \times P_{ij}\tilde{e}_j] \tag{12}$$

and of the entropy

$$\frac{\partial(\rho s)}{\partial t} + div(\tilde{j}_m s) = -div\Big(\frac{\tilde{q}}{T}\Big) + X. \tag{13}$$

Here $(\vec{j}_m \otimes \vec{u})$ is the second rank tensor obtained as a direct product of the vectors $\vec{j}_m$ and $\vec{u}$. When we take the divergence of the second rank tensor, we carry out the contraction with respect to its first index. The symbol P_{ij} in the equation (12) means the portrait of the tensor P in the basis $(\vec{e}_1, \vec{e}_2, \vec{e}_3)$. The summation is carried out with respect to the indexes i and j that appear twice.

The system (9)–(13) is not closed. It is necessary to introduce the variables $\vec{j}_m$, P, $\vec{q}$, $\vec{A}$, X as the functions of macroscopic parameters of the medium and their derivatives. The closure problem can be solved in several ways.

2.3 The classical approach to the closure problem. The Navier–Stokes equations

First of all let us discuss the classical approach [12], in which the averaging over a certain set of physically infinitely small volumes from the space $R_{\vec{x}}^3$ at the fixed moment of time t is used for definition of hydrodynamic variables. In this case the mass flow density vector $\vec{j}_m$ at the arbitrary

point $(\vec{x}, t)$ coincides with the average momentum of the unit volume $\rho\vec{u}$, so the first closure relation looks as follows:

$$\vec{j}_m = \rho\vec{u}. \tag{14}$$

After that the pressure and inner viscous friction forces are introduced. They act instantly on the surface of the material volume. The law of motion of the latter is chosen in the same way as in the rigid body mechanics. In literature this assumption is called the solidification principle. The balance equation for the angular momentum (12) follows from the momentum conservation law (10) and the symmetry of the tension tensor P. In the theory for Newtonian media $P = P_{NS}$ is defined by the expression

$$P = \Pi_{NS} - pI, \tag{15}$$

where

$$\Pi_{NS} = \eta[(\vec{\nabla}\otimes\vec{u}) + (\vec{\nabla}\otimes\vec{u})^T - (2/3)I\,div\,\tilde{u}] \tag{16}$$

– is the Navier-Stokes shear-stress tensor, I – the unit tensor – is the invariant of the second range. The heat flow $\vec{q} = \vec{q}_{NS}$ is defined according to the Fourier law

$$\vec{q} = -\ae\tilde{\nabla}\,T. \tag{17}$$

The hypothesis (16) and (17) for the ideal monoatomic gases with small Knudsen numbers are confirmed by the kinetic computations. The work of the surface pressure forces and inner viscous shear-stress forces in a unit of time is computed using the same formula as in the rigid body mechanics, that is:

$$\vec{A} = (P_{NS}\cdot\vec{u}). \tag{18}$$

The specific thermodynamical entropy is supposed to satisfy the Gibbs differential identity

$$T\,ds = d\varepsilon + p\,d(1/\rho). \tag{19}$$

Its balance equation (13) may be obtained as a consequence of the mass, momentum and energy conservation laws (10)–(11), if we choose $X = X_{NS}$ as

$$X = \ae\left(\frac{\tilde{\nabla}\,T}{T}\right)^2 + \frac{(\Pi_{NS} : \Pi_{NS})}{2\eta\,T}, \tag{20}$$

where $(\Pi_{NS} : \Pi_{NS}) = \sum_{i,j=1}^{3}(\Pi_{NS})_{ij}(\Pi_{NS})_{ij}$ – is the double dot product of two identical tensors. Note that the right hand side of the equality (20) is non-negative. Substitution of the expressions (14)–(18) into equations (9) – (10) gives us the classical Navier-Stokes system. The dependensies $\eta = \eta(\rho, T)$ and $\ae = \ae(\rho, T)$ may be either found experimentally or derived from the kinetic theory of gases.

2.4 The non-traditional approach to the closure problem. The quasi-hydrodynamic system

Another way of solving the problem of closing the system (9)–(13) was proposed by Yu.V.Sheretov in [1], [2]. To define hydrodynamic variables he used not the spatial, but the time-spatial averaging over a certain set of physically infinitely small four-dimensional volumes in the space $R^4_{\vec{x},t}$. He has proved that in the case of such time-spatial averaging the mass flow density vector $\vec{j}_m$, generally speaking, doesn't coincide with the average momentum of the unit volume $\rho\vec{u}$. Detailed analysis of different possibilities for choosing the variables $\vec{j}_m$, P, $\vec{q}$, $\vec{A}$ X gave the following result:

$$\vec{j}_m = \rho(\vec{u} - \vec{w}), \tag{21}$$

$$P = -pI + \Pi_{NS} + \rho\vec{u}\otimes\vec{w}, \tag{22}$$

$$\vec{q} = -\ae\tilde{\nabla}\,T, \tag{23}$$

$$\vec{A} = (\Pi_{NS} \cdot \vec{u}) + \rho\vec{u}(\vec{w} \cdot \vec{u}) - p(\vec{u} - \vec{w}), \tag{24}$$

$$X = \text{æ}\Big(\frac{\tilde{\nabla} T}{T}\Big)^2 + \frac{(\Pi_{NS} : \Pi_{NS})}{2\eta T} + \frac{\rho\tilde{w}^2}{\tau T}, \tag{25}$$

where

$$\vec{w} = \frac{\tau}{\rho}[\rho(\vec{u} \cdot \vec{\nabla})\vec{u} + \vec{\nabla} p - \rho\vec{F}]. \tag{26}$$

The parameter $\tau = \tau(\rho, T)$ describes the scale of temporal smoothing. The formula for computing this parameter was proposed in [2]:

$$\tau = \frac{\gamma}{Sc}\frac{\eta}{\rho c_s^2}, \tag{27}$$

where γ is the isentropic exponent, Sc is the Schmidt number (which is close to 1 for gases), c_s is the sound velocity. The value of τ agrees by order with the average mean free path of the particles in gas. Computations for moderately rarified gases confirm the correctness of this choice of the smoothing parameter [3].

Having substituted the expressions (21), (22) and (24) instead of $\vec{j}_m$, P and $\vec{A}$ in (9)–(11), we obtain the quasi-hydrodynamic (QHD) system of equations:

$$\frac{\partial\rho}{\partial t} + div(\rho\tilde{u}) = div(\rho\tilde{w}), \tag{28}$$

$$\frac{\partial(\rho\vec{u})}{\partial t} + div(\rho\tilde{u} \otimes \tilde{u}) + \tilde{\nabla} p = \rho\tilde{F} + div\,\Pi_{NS} + div[(\rho\tilde{w} \otimes \tilde{u}) + (\rho\tilde{u} \otimes \tilde{w})], \tag{29}$$

$$\frac{\partial}{\partial t}\Big[\rho\Big(\frac{\vec{u}^2}{2} + \varepsilon\Big)\Big] + div\Big[\rho\tilde{u}\Big(\frac{\tilde{u}^2}{2} + \varepsilon\Big) + p\tilde{u}\Big] + div\,\tilde{q} = \rho\tilde{F} \cdot (\tilde{u} - \tilde{w}) +$$
$$+ div(\Pi_{NS} \cdot \tilde{u}) + div\Big[\rho\tilde{w}\Big(\frac{\tilde{u}^2}{2} + \varepsilon\Big) + p\tilde{w} + \rho\tilde{u}(\tilde{w} \cdot \tilde{u})\Big]. \tag{30}$$

The QHD system (28)–(30) becomes closed if it is equipped with the state equations (1), and the coefficients η, æ and τ are presented as functions of macroscopic parameters of the media. The substitution of the expressions (21), (23) and (25) into (13) gives the entropy balance equation

$$\frac{\partial(\rho s)}{\partial t} + div(\rho\tilde{u}s) = div(\rho\tilde{w}s) + div\Big(\text{æ}\frac{\tilde{\nabla} T}{T}\Big) + \text{æ}\Big(\frac{\tilde{\nabla} T}{T}\Big)^2 + \frac{\Psi_{QHD}}{T}, \tag{31}$$

in which

$$\Psi_{QHD} = \frac{(\Pi_{NS} : \Pi_{NS})}{2\eta} + \frac{\rho\vec{w}^2}{\tau}$$

is the non-negative dissipative function.

A number of theoretical results is obtained for the QHD system (28)–(30) in [1], [2]. In particular, it has been shown that the stationary QHD system in dimensionless variables differs from the corresponding Navier-Stokes equations only in terms of the second order of magnitude with respect to the Knudsen number. Its laminar boundary layer approximation is the classical Prandtl system.

2.5   Quasi-hydrodynamic system for a viscous incompressible fluid

In many particular cases of hydrodynamic flows we may neglect the density variation. Supposing that ρ and T are constant, from the equations (28), (29) we obtain the system

$$div\,\tilde{u} = div\,\tilde{w}, \tag{32}$$

$$\frac{\partial \vec{u}}{\partial t} + div(\tilde{u} \otimes \tilde{u}) + \frac{1}{\rho}\tilde{\nabla}p = \tilde{F} + \frac{1}{\rho}div\,\Pi_{NS} + div\left[(\tilde{w} \otimes \tilde{u}) + (\tilde{u} \otimes \tilde{w})\right], \qquad (33)$$

which is closed with respect to the unknown functions - the velocity $\vec{u} = \vec{u}(\vec{x}, t)$ and the pressure $p = p(\vec{x}, t)$. Here the vector
$\vec{w}$ is defined by formula

$$\vec{w} = \tau\left((\vec{u} \cdot \vec{\nabla})\vec{u} + \frac{1}{\rho}\vec{\nabla}p - \vec{F}\right).$$

We shall compute the tensor Π_{NS} using the expression

$$\Pi_{NS} = \eta[(\vec{\nabla} \otimes \vec{u}) + (\vec{\nabla} \otimes \vec{u})^T].$$

The coefficient of dynamical viscosity η and the characteristic time τ are considered to be given positive constants. Taking the formal limits in (32)–(33) as $\tau \to 0$, we get the classical Navier-Stokes equations that describe the viscous non-compressible flows. The system (32)–(33) is dissipative and possesses several explicit and physically reasonable solutions [1]–[4]. The particular case of plane or spatial axially symmetric isothermal flows without external forces $\vec{F} = 0$ gives

$$\frac{\partial u_x}{\partial x} + \frac{1}{y^k}\frac{\partial(y^k u_y)}{\partial y} = \frac{\partial w_x}{\partial x} + \frac{1}{y^k}\frac{\partial(y^k w_y)}{\partial y}, \qquad (34)$$

$$\frac{\partial u_x}{\partial t} + \frac{\partial(u_x^2)}{\partial x} + \frac{1}{y^k}\frac{\partial(y^k u_y u_x)}{\partial y} + \frac{1}{\rho}\frac{\partial p}{\partial x} =$$
$$= 2\frac{\partial}{\partial x}\left(\nu\frac{\partial u_x}{\partial x}\right) + \frac{1}{y^k}\frac{\partial}{\partial y}\left[y^k\nu\left(\frac{\partial u_x}{\partial y} + \frac{\partial u_y}{\partial x}\right)\right] +$$
$$+ 2\frac{\partial(u_x w_x)}{\partial x} + \frac{1}{y^k}\frac{\partial(y^k u_y w_x)}{\partial y} + \frac{1}{y^k}\frac{\partial(y^k u_x w_y)}{\partial y}, \qquad (35)$$

$$\frac{\partial u_y}{\partial t} + \frac{\partial(u_x u_y)}{\partial x} + \frac{1}{y^k}\frac{\partial(y^k u_y^2)}{\partial y} + \frac{1}{\rho}\frac{\partial p}{\partial y} =$$
$$= \frac{\partial}{\partial x}\left[\nu\left(\frac{\partial u_x}{\partial y} + \frac{\partial u_y}{\partial x}\right)\right] + \frac{2}{y^k}\frac{\partial}{\partial y}\left(y^k\nu\frac{\partial u_y}{\partial y}\right) - 2k\nu\frac{u_y}{y^2} +$$
$$+ \frac{\partial(u_x w_y)}{\partial x} + \frac{\partial(u_y w_x)}{\partial x} + \frac{2}{y^k}\frac{\partial(y^k u_y w_y)}{\partial y}, \qquad (36)$$

where
$$w_x = \tau\left(u_x\frac{\partial u_x}{\partial x} + u_y\frac{\partial u_x}{\partial y} + \frac{1}{\rho}\frac{\partial p}{\partial x}\right), \quad w_y = \tau\left(u_x\frac{\partial u_y}{\partial x} + u_y\frac{\partial u_y}{\partial y} + \frac{1}{\rho}\frac{\partial p}{\partial y}\right).$$

Here $\nu = \eta/\rho$ is the coefficient of kinematic viscosity, the parameter k equals to zero in the plane case and equals to one in the axially symmetric one. The unknown variables are the components of the velocity $u_y = u_y(x, y, t)$, $u_x = u_x(x, y, t)$ with respect to the ortonornal local basis $(\vec{e}_x, \vec{e}_y)$ and the pressure $p = p(x, y, t)$. The pressure field is defined using the already found fields of velocity and temperature by solving the Poisson equation:

$$\frac{1}{\rho}\left[\frac{\partial^2 p}{\partial x^2} + \frac{1}{y^k}\frac{\partial}{\partial y}\left(y^k\frac{\partial p}{\partial y}\right)\right] = \frac{1}{\tau}\left[\frac{\partial u_x}{\partial x} + \frac{1}{y^k}\frac{\partial(y^k u_y)}{\partial y}\right] -$$
$$- \frac{\partial}{\partial x}\left(u_x\frac{\partial u_x}{\partial x} + u_y\frac{\partial u_x}{\partial y}\right) - \frac{1}{y^k}\frac{\partial}{\partial y}\left[y^k\left(u_x\frac{\partial u_y}{\partial x} + u_y\frac{\partial u_y}{\partial y}\right)\right], \qquad (37)$$

This equation is the equivalent representation of (34) when $\tau = const$.

3   Problem statement and computational algorithm

Let us consider a plane two-dimensional incompressible flow in the channel of height H and of length L with small Mach numbers. The channel has a narrowing at the entrance section. The size of the narrowing is determined by the height of the step h. The scheme of the computational domain and the forming flow are demonstrated in Fig.1.
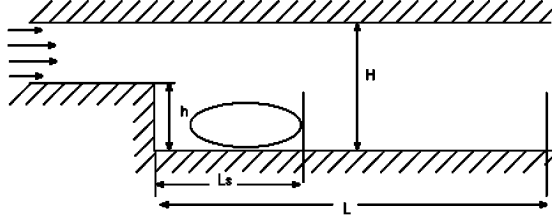

Figure 1: Scheme of the computational domain

We use the QHD system (34)–(36) with $k = 0$ as the mathematical model. We transform this system into the dimensionless form, applying the relations

$$x = \tilde{x}H, \quad y = \tilde{y}H, \quad u_x = \tilde{u}_x U_0, \quad u_y = \tilde{u}_y U_0, \quad p = \tilde{p}\rho U_0^2, \quad t = (\tilde{t}H)/U_0, \quad Re = (U_0 H)/\nu,$$

where

$$U_0 = \frac{1}{H-h} \int_h^H u_0(y)dy$$

is the flow velocity in the channel, averaged over the section, and $u_0(y)$ is the given velocity profile at the entrance section. We equip this dimensionless system with boundary conditions
  • the solid lower wall

$$y = 0, \quad 0 < x < L/H, \quad u_x = u_y = 0, \quad \frac{\partial p}{\partial y} = 0;$$

  • the solid upper wall

$$y = 1, \quad 0 < x < L/H, \quad u_x = u_y = 0, \quad \frac{\partial p}{\partial y} = 0;$$

  • the solid left wall

$$x = 0, \quad 0 < y < h/H, \quad u_x = u_y = 0, \quad \frac{\partial p}{\partial x} = 0;$$

  • the inflow region at the left boundary

$$x = 0, \quad h/H < y < 1, \quad u_x = u_0(y), \quad u_y = 0, \quad \frac{\partial p}{\partial x} = const;$$

  • the right boundary

$$x = L/H, \quad 0 < y < 1, \quad \frac{\partial u_x}{\partial x} = \frac{\partial u_y}{\partial x} = 0, \quad p = 0.$$

Pressure boundary condition at the solid walls follows from the non-flow conditions for the velocity components and from the impermeability condition for the mass flow $\vec{j}_m$ (21). The pressure gradient at the channel entrance may be taken arbitrary. For example, it is possible to compute its values in the following way: we set the velocity profile at the channel entrance as the Poiseuille parabola [12], [13]:

$$u_0(y) = \frac{Re}{2}\frac{\partial p}{\partial x}(1 - y)(h/H - y). \tag{38}$$

The mass flow rate at the entrance section is computed according to the following formula

$$J = \int_{h/H}^{1} [u_x(0,y) - w_x(0,y)]dy = -\frac{Re}{12}(1 - h/H)^3\frac{\partial p}{\partial x} - \tau(1 - h/H)\frac{\partial p}{\partial x}. \qquad (39)$$

From (39) we find

$$\frac{\partial p}{\partial x} = -\frac{12J}{Re(1 - h/H)^3}\left[1 + \frac{12\tau}{Re(1 - h/H)^2}\right]^{-1}. \qquad (40)$$

We chose the initial condition: $u_x = u_y = 0$. The pressure gradient at the initial moment was supposed to be constant all over the flow field.

The dimensionless smoothing parameter τ for laminar flows (27) was taken equal to

$$\tau = \frac{\gamma}{Sc}\frac{Ma}{Re_s} + \tau_0, \text{ where } Ma = \frac{U_0}{c_s}, \; Re_s = \frac{c_s H}{\nu} \qquad (41)$$

- are the Mach number and the Reynolds number, derived from the speed of sound. For example, the air at normal temperature yields $c_s = 3.4 \cdot 10^4$ /, $\nu = 0.15^2$/c, $H = 10$, $Re_s = 2 \cdot 10^6$. For laminar flows we have $Ma << 1$. So for real flows the smoothing parameter proves to be small. We added to it the value τ_0 in order to compensate the difference scheme's antidiffusion and to provide stable computing. The value of τ_0 was chosen proportional to $1/Re$.

The QHD equations are solved numerically using the algorithm, similar to the one described in [4]–[6], - the explicit finite- difference scheme with second order of accuracy with respect to all spatial variables. Velocity and pressure values are defined in the same grid points. At each time step, the pressure field is calculated by using the velocity field, as a solution of Poisson equation (37), which is also approximated with the second order space accuracy. The Poisson equation is solved by the preconditioned generalized conjugate gradient method.

To present the numerical results, let us also introduce the stream-function, which is related to the solenoidal field $\vec{u} - \vec{w}$. These relations [12] look as follows:

$$u_y - w_y = -\frac{1}{y^k}\frac{\partial \psi}{\partial x}, \quad u_x - w_x = \frac{1}{y^k}\frac{\partial \psi}{\partial y}. \qquad (42)$$

The boundary conditions for the stream-function are defined as follows - At the lower boundary of the computational domain and at the left wall we use the normalization $\psi = 0$, because there we have the impermeable boundary conditions. At the upper boundary the stream-function equals to the mass flow rate of the liquid.

4 Numerical modeling of laminar flows

For proper verification of the numerical method for back-step flow the problem described above has been solved with Re=100, 200, 300, 400; $h/H = 1/2$. (From here on the Reynolds number is evaluated using the height of the step). The velocity profile at the entrance section represented the Poiseuille's parabola (38). The dimensionless liquid mass flow rate J was taken equal to 1; it corresponded to the choice of the entrance pressure gradient in form of

$$\frac{\partial p}{\partial x} = -\frac{96}{Re}\left[1 + \frac{48\tau}{Re}\right]^{-1}.$$

For the small values of τ and the big values of Re we may suppose that

$$\frac{\partial p}{\partial x} = -\frac{96}{Re}.$$

The computed length of the separation zone behind the step was compared with data from [8]. It was also defined from graphs presented in [10].

In [8] the Reynolds number was derived from the average flow velocity and from the height of the step. The entrance profile was also set in form of the Poiseuille's parabola. The mass flow

rate J was taken equal to 1. The results, in particular, contain the length of the separation zone for $H = 2h$, $Re(h)$=100, 200, 300. In [10] the Reynolds number was derived from the value of $2h$ and the average entrance velocity. Graphic data concerning the length of the separation zone for $50 < Re(2h) < 800$ are presented here.

The results, obtained by authors, are systematized in the table 1. Here L is the dimensionless length of the computational domain, N_x, N_y are the numbers of mesh points in both directions, L_s is the length of the separation zone, N_{iter} is the number of time steps till the conversion is achieved. The spatial mesh is uniform in both directions with equal widths $h_x = h_y = 0.025$. It is well known that the usage of equal widths h_x and h_y improves the accuracy of description of the separating flow.

We have $Re_s \sim 10^6$ in the described flows, so the value $\tau = \tau_0$ in (41)was taken equal to $\tau_0 = 0.5/Re$. The time step δt was equal to 10^{-4} for all variants of computation.

$Re(h)$	100	200	300	400
L	7.5	5.0	7.5	10
$N_x \times N_y$	300×40	200×40	300×40	400×40
τ	0.005	0.0025	0.00166	0.00125
N_{iter}	19800	~ 20000	~ 60000	~ 110000
L_s/h present comp	5.0	8.2	10.1	14.8
L_s/h [8], comput	4.43	7.5	10.0	-
L_s/h [10] exp	5.0	8.5	11.3	14.2
L_s/h [10] comput	5.0	8.3	8.4	7.8

Table 1: Computations of laminar flows

Computation stops when the condition $\delta p < 10^{-3}$ is satisfied.

$$\delta p = \max \left| \frac{p^{n+1} - p^n}{\delta t} \right|,$$

n is the time step number.

In all variants the flow reaches the stationary regime. The length of the separation zone L_s was defined by the location of the zero stream-function line. It is indicated with the accuracy 0.2. Comparison of the results mentioned above with corresponding data from the Navier-Stokes simulation and with the experiments [10] demonstrates good agreement both in the length of the separation zone and in the picture of the flow in general. Mention, the good agreement for QHD and experimental results for Re = 400. An almost linear increase of the values of L_s is observed in computations with the increasing number Re.

For Re = 100 and 200 the process of flow relaxation consists of the appearence and further growth of a single vortex behind the step. For Re = 300 and 400 this process proves to be oscillatory and is accompanied with arising and separation of vortex-like formations, but, unlike the regimes with greater Reynolds numbers (they are considered in the second part of this paper), this oscillations fade and finally form a single stationary vortex behind the step. The isolines of the flow function ψ, constructed according to (42), are demonstrated in Figs. 2, 3. They illustrate the process of flow relaxation in time for $Re = 100$ and 400. The isolines are placed equidistantly.

With further increasing of the Reynolds number the stationary solution becomes unstable.

The influence of the regularization parameter τ and the conversion of the numerical solution was investigated for the variant with $Re = 100$. The value of τ was additionally chosen equal to $5 \cdot 10^{-4}$ and $5 \cdot 10^{-2}$; the time step δt was changed proportionally.

Besides the mesh described in the table, we also used another one - with twice as many nodes in both directions. The decreasing of the spatial mesh size by factor of two caused the analogous decreasing of the time step. It was shown that the length of the separation zone and the general picture of the flow practically doesn't depend neither of the value of regularization parameter τ nor of the spatial mesh widths h_x and h_y. The increasing of τ causes smoothing of the flow picture
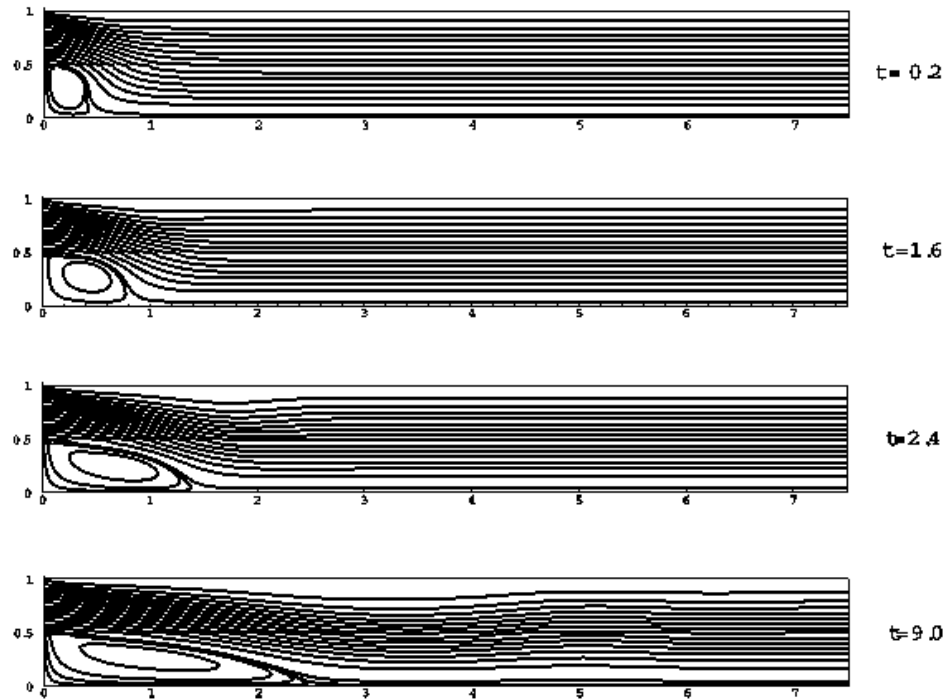
Figure 2: Stream functions for Re=100
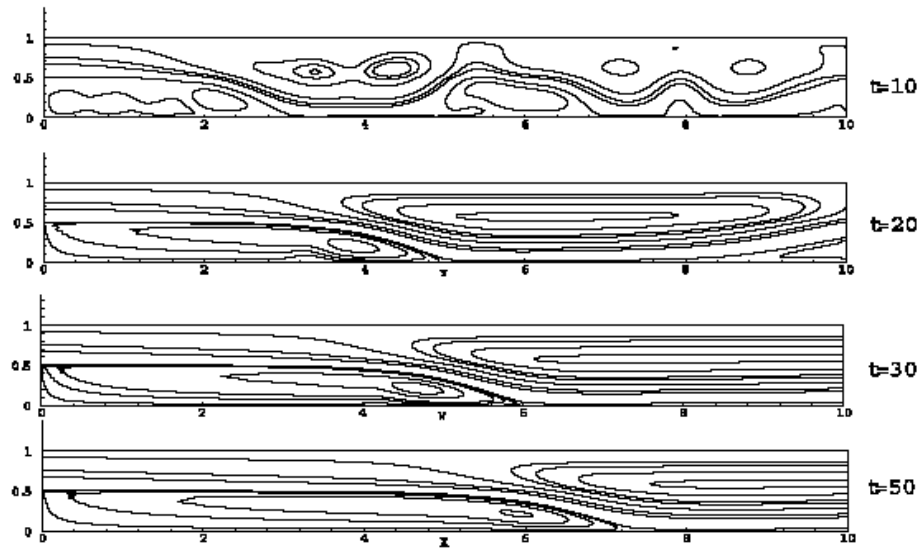

Figure 3: Stream functions for Re=400

and allows us to increase the time step. Spatial mesh refinement gives a more detailed picture of the flow.

We have studied the dependence of the solution on the pressure gradient at the entrance section with the average velocity and mass flow rate remaining constant. It was found out that the pressure gradient variation in the range from $-96/Re$ to $-12/Re$ practically doesn't influence the structure of the flow: at the distance around $0.5h$ from the entrance boundary the pressure adjusts to the existing liquid mass flow rate and practically doesn't depend on the initial gradient.

5 Conclusion

The present paper contains the phenomenological derivation of quasi-hydrodynamic equations. Two-dimensional mathematical model describing the viscous incompressible flow behind the back step is formulated and solved numerically.

The computer simulation shows that the flows with small Reynolds numbers that correspond to the laminar regime, are stationary. The obtained regimes are in good agreement with the corresponding solutions of the Navier-Stokes system and with experimental data mentioned in literature. Oscillations that appear in the solutions describing the relaxation of laminar flows for moderate Reynolds numbers, fade with time. The final flow doesn't depend on the choice of the smoothing parameter τ, which plays the role of regularizator in these computations.

These results are in consistence with theoretical estimates [2]. According to them, additional QHD-terms should be small in case of stationary flows and the solution of the QHD system is expected to be close to the solution of the Navier-Stokes system. Additional terms act as the regularizators and allow us to apply a relatively simple, stable and accurate numerical algorithm.

The authors acknowledge Laboratoire D'Aerothermique du CNRS, Orleans, and personally Dr. J.-C. Lengrand, for the permanent support of this research.

References

[1] Sheretov Yu.V. Quasi-hydrodynamic equations as a model for viscous compressible heat conductive flows. Application of functional analysis in the theory of approximations. Tver University, 1997 P. 127–155 (in Russian).

[2] Sheretov Yu.V. Mathematical modeling of gas and liquid flows basing on Quasi-hydrodynamic and quasi-gas-dynamic equations. Tver, Tver Statet University, 2000 (in Russian).

[3] Elizarova T.G., Sheretov Yu.V. Analyse du probleme de l'ecoulement gazeux dans les microcanaux par les equations quasi hydrodynamiques. Journal "La Houille Blanche Revue Internationale de l'Eau", 2003, No 5, pp. 66 - 72.

[4] Elizarova T.G., Sheretov Yu.V. Theoretical and numerical investigation of quasi-gas-dynamic and quasi-hydrodynamic equations. Comput. Mathem. and Mathem. Phys. 2001. V. 41. N 2. P. 219–234.

[5] Gurov D.B., Elizarova T.G., Sheretov Yu.V. Numerical simulation of fluid flow in a cavity based on the quasi-hydrodynamic system of equations. J. Mathem. Modelirovanie, 1996, vol.8, No 7, pp.33 - 44 (in Russian)

[6] Elizarova T.G., Kalachinskaya I.S., Kluchnikova A.V., Sheretov Yu.V., (1998), Application of Quasi-Hydrodynamic equations in the Modeling of Low-Prandtl Thermal Convection. Comput. Mathem. and Math. Phys., 1998, Vol.38, No.10, pp. 1662 – 1671.

[7] Elizarova T.G., Milyukova O.Yu. Numerical Simulation of Viscous Incompressible Flow in a Cubic Cavity. Comp.Mathem. and Math. Phys., 2003, Vol.43, No 3., pp.453 - 466.

[8] Sparrow E.M., Chuck W. PC solutions for heat transfer and fluid flow downstream of an abrupt, asymmetric enlargement in a channel. Numer. Heat Transfer. V. 12. P. 19–40, 1987.

[9] Kim J., Moin P. Application of a fractional–step method to incompressible Navier–Stokes equations. J. of Comput. Phys. V. 59. P. 308–323, 1985.

[10] Armaly B.F., Durst F., Pereira J.C.F., Schonung B. Experimental and theoretical investigation of backward–facing step flow. J. of Fluid Mech. V. 127. P. 473–496, 1983.

[11] Hackman L.P., Raithby G.D., Strong A.B. Numerical predictions of flows over backward–facing steps. Intern. J. for Numer. Meth. in Fluids. V. 4. N 8. P. 711–724, 1984.

[12] Loitsyanskii L.G. Mechanics of liquids and Gases. Ed. Nauka, Moscow, 1987 (in Russian)

[13] Landau L.D., Lifshitz E.M. Hydrodynamics, Ed. Nauka, Moscow, 1986 (in Russian)

[14] Elizarova T.G, Kalachinskaya I.S., Weber R, Hureau J., Lengrand J.-C. (2001) Ecoulement derriere une marche. Etude experimentale et numerique. Laboratoire d'Aérothermique du CNRS, Orleans (Fr), R 2001 - 1.